

Ingot Metallurgy Aluminum-Lithium Alloys for Aircraft Structure

J.C. Ekvall* and D.J. Chellman†

Lockheed-California Company, Burbank, California

Aluminum-lithium (Al-Li) alloys are undergoing intensive development as replacements for conventional aluminum alloy materials in aircraft structural applications. The reported material property behavior demonstrates that the strength and fracture toughness properties are comparable to 7075-T6X aluminum alloys. The strength, ductility, and toughness combination of Al-Li alloys can be varied by changing heat treatment and thermal mechanical history. Initial property results were obtained from coupon tests on extruded bar materials and compared to baseline 7075-T6X aluminum. The structural behavior was demonstrated by static tests conducted on lugs, typical of those used in airframe applications. Experimental findings and predictions are discussed in terms of Al-Li material properties. An analysis by structural failure modes, e.g., tension, compression, etc., shows a potential weight savings of 7-17% for individual Al-Li structural components. When applied to an entire fighter aircraft configuration, the weight savings potential is approximately 9.5%.

Nomenclature

D	= lug hole diameter, in.
e	= tensile elongation, %
E	= modulus of elasticity, $\times 10^6$ psi
E_s	= secant modulus of elasticity, $\times 10^6$ psi
F	= durability and damage tolerance assessment stress allowable, ksi
F_{cy}	= compression yield strength, ksi
F_{su}	= ultimate shear strength, ksi
F_{tu}	= ultimate tensile strength, ksi
F_{ty}	= 0.2% tensile yield strength, ksi
K_{BR}	= bearing efficiency factor, dimensionless
K_Q	= conditional plane-strain fracture toughness, ksi-in. ^{1/2}
K_{tb}	= peak tension stress at lug hole divided by average bearing stress, dimensionless
L	= longitudinal extrusion direction
LT	= long-transverse extrusion direction
ST	= short-transverse extrusion direction
P	= applied load, lb
P_{ult}	= failure load of lug, lb
R_0	= radius at end of tapered lug, in.
t	= lug thickness, in.
-T3X	= naturally aged heat treatment temper
-T8X	= artificially aged heat treatment temper
W	= structural weight, lb
Δ	= pin deflection in direction of applied load, in.
θ	= loading angle, deg
ρ	= material density, lb/in. ³

Subscripts

1	= 7075-T6X aluminum alloys
2	= aluminum-lithium alloys

Introduction

THE renewed interest in low-density Al-Li alloys stems from weight savings analyses and parametric design studies performed by the aerospace industry in the late 1970s.¹ These findings showed that a reduction in alloy density is more effective in improving performance and fuel economy than commensurate improvements in any other single primary property, such as strength or modulus, or second-tier properties, such as toughness or fatigue. In the same time period, several major aluminum producers in the United States, England, and France started developing an advanced ingot-casting technology for lithium containing aluminum alloys. The community of aluminum producers and aerospace users are now actively pursuing the development and introduction of low-density Al-Li alloy materials for aircraft structural applications.

Alloying and processing development activities to support the anticipated need for Al-Li alloy materials are currently underway at the major aluminum suppliers. A number of alloy products and heat treatment tempers have been announced and scheduled for delivery to the aircraft industry. However, only limited quantities of material have been available for property evaluations to date. In recognition of this situation, the Lockheed-California Company, in cooperation with Naval Surface Weapons Center (NSWC), initiated a series of development studies to identify promising Al-Li alloys for structural applications. One such candidate alloy, suitable for replacing conventional 7075-T6X aluminum, was cast and fabricated into the wrought product forms shown in Fig. 1.

A considerable amount of coupon, element, and component testing is required to qualify a new material for aircraft structural applications. These data are necessary to characterize the material properties, to establish design material properties, and to provide assurance that structures can meet strength and other design requirements. Coupon tests were conducted to define the static strength properties of the LOCKALITE alloy. To evaluate the material for structural applications, some lugs, typical of those used on landing gears, actuators, and control surface structures, were designed and tested. Some of the results obtained from these tests are described in this paper.

Received March 20, 1986; presented as Paper 86-0890 at the AIAA/ASME/ASCE/AHS 27th Structures, Structural Dynamics, and Materials Conference, San Antonio, TX, May 19-21, 1986; revision received Sept. 22, 1986. Copyright © 1987 by Lockheed-California Company. Published by the American Institute of Aeronautics and Astronautics, Inc. All rights reserved.

*Research and Development Engineer, Advanced Structures Department. Member AIAA.

†Research Specialist, Materials and Processes Department.

Material Development

The Lockheed-California Company has been involved in the development and evaluation of Al-Li alloy materials since 1978. Recent laboratory scale studies, in cooperation with NSWC,² have led to the identification of several candidate alloy systems that represent replacements for conventional 2024-T3X, 7075-T6X, and 7075-T73X aluminum alloys. In the present effort, an Al-Li alloy exhibiting strength/ductility/toughness combinations which are competitive with a 7075-T6X alloy is described with respect to materials characterization and structural performance for aircraft lug applications.

Material Fabrication

An Al-Li alloy with the composition Al-2.1Li-2.5Cu-1.0Mg-0.13Zr (designated LOCKALITE) offers the advantage of a 7.5% decrease in density and a 12.5% increase in elastic modulus when compared to 7075-T6X aluminum. In 1984, a 1000-lb, 12.0-in.-diam \times 106.0-in.-long ingot was cast of the LOCKALITE composition at International Light Metals, Inc. (formerly Martin-Marietta Aluminum) in its Torrance, CA, facility. Chemical analyses indicated that the target composition was achieved in the billet. A homogenization treatment at 975°F for 12 h was used to minimize solute segregation prior to final hot working. The five product forms shown in Fig. 1 were subsequently processed from the LOCKALITE ingot. The extrusion products represent the first Al-Li-shaped extrusions available to Lockheed for test and evaluation. The forged fitting represents a near-net shape part common in structural applications in the

aerospace industry. In general, the LOCKALITE alloy exhibited excellent workability, and the resultant wrought products were visually equivalent to conventional high-strength aluminum alloys.

Heat Treatment Studies

The 1.0 \times 4.0-in. rectangular bar was extruded at approximately 750°F from a 10.5-in.-diam billet, resulting in an extrusion ratio of 22:1. Differential scanning calorimetry measurements were conducted on the LOCKALITE material to determine an optimum solution treatment practice. Solution heat treatment at 990°F for 2 h was employed to ensure that all alloying elements were in complete solid solution. The extrusions were stretched a nominal 2.5%, immediately following solution treatment and cold-water quench, prior to any age hardening. An isothermal aging study as a function of temperature and time was conducted initially to identify candidate heat treatment tempers (Fig. 2). Tensile tests were conducted on heat treatments that corresponded to under-aged, peak-aged (-T8X), and over-aged portions of the precipitation hardening curves, in addition to the naturally aged condition (-T3X). The artificial aging temperatures under evaluation ranged from 300 to 400°F. These tensile property screening results led to the selection of a recommended -T8X temper consisting of 350°F for 24 h.³ For this heat treatment condition, an optimum combination of strength and ductility was obtained in the LOCKALITE alloy extrusions.

Table 1 Summary of property behavior comparisons for selected IM Al-Li alloy extrusions

Material property	LOCKALITE alloy	ZZZA alloy	ZZZB alloy	7075-T6 alloy	Goal
F_u , ksi					
L	88,400	80,600	87,100	81,000	85,000
LT	79,100	71,200	79,400	—	—
F_y , ksi					
L	83,000	75,300	83,100	72,000	77,500
LT	70,300	61,900	73,300	—	—
Elongation, %					
L	9.1	6.6	7.0	7.5	10.0
LT	8.3	5.8	6.2	—	—
K_Q , ksi-in. ^{1/2}					
L-T	32.7	35.1	19.0	27.5	25.0
T-L	28.4	21.9	12.2	—	—

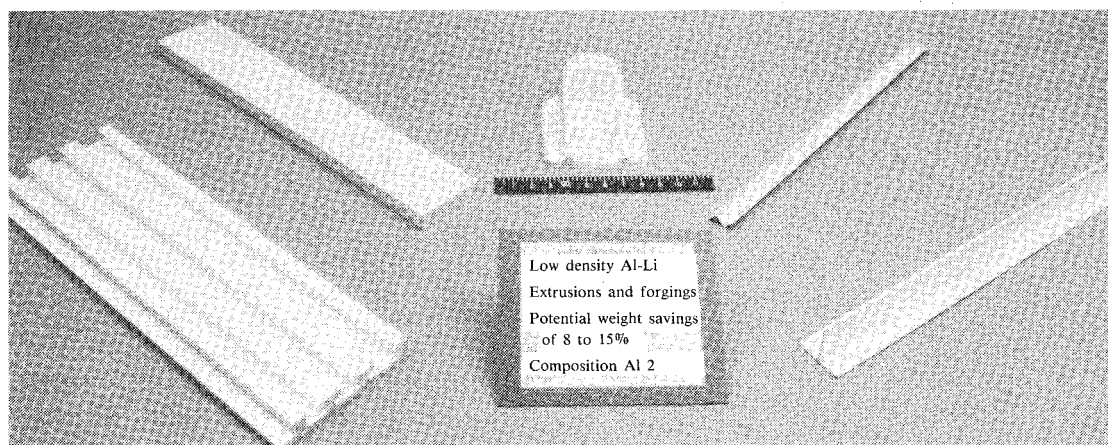
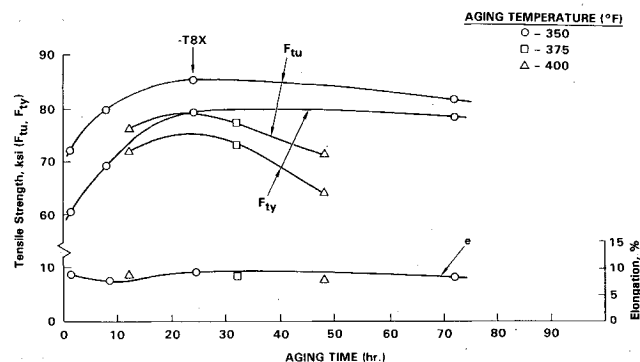


Fig. 1 Extrusion and forging products fabricated in IM Al-Li-X alloy (LOCKALITE) study.

Table 2 Comparison of tensile and shear properties for extruded bars used in lug specimens

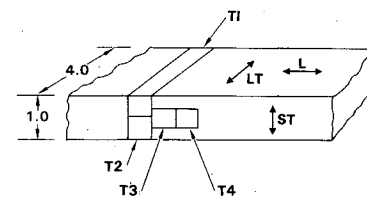
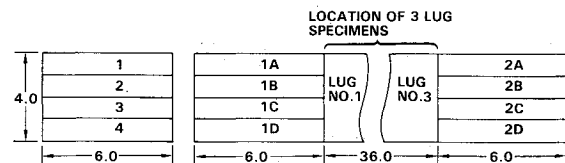
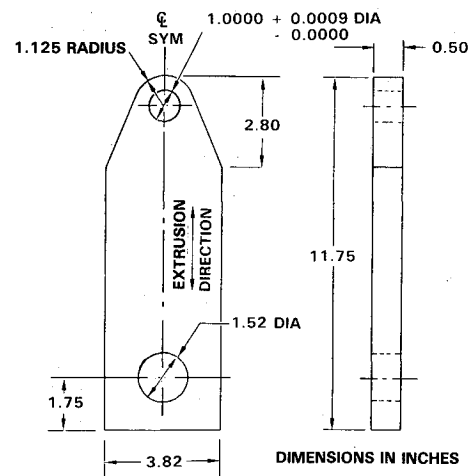
Material property	Location of material	Al-Li-X alloy	7075-T6 alloy ^a
F_{tu} , ksi			
L	edge	91,100	85,000
L	center	84,400	85,000
LT	surface	80,800	78,000
LT	center	76,400	78,000
F_{ty} , ksi			
L	edge	87,200	76,000
L	center	79,200	76,000
LT	surface	71,600	68,000
LT	center	67,500	68,000
Elongation, %			
L	edge	5.9	7
L	center	9.1	7
LT	surface	6.5	7
LT	center	7.0	7
F_{su} , ksi			
L	center	42,200	40,700
LT	center	42,400	43,400
ST	center	33,200	43,200

^aTensile properties from Ref. 4. Shear properties based on average of 3 tests from 7075-T6 rectangular extrusion.

**Fig. 2 Isothermal aging response for IM Al-Li-X alloy (LOCKALITE) extrusions.**

Material Properties

A property test evaluation was performed on the LOCKALITE extruded bar, as well as on two commercial alloys. The two alloy extrusions, designated ZZZA and ZZZB, were procured from British Alcan Aluminum Limited and were evaluated as part of an internal study on advanced metallic materials. Tensile test results for the various low-density Al-Li-X alloy extrusions are shown in Table 1. Tests were conducted in both the L and LT extrusion orientations and were compared with properties for 7075-T6X aluminum extrusions obtained from MIL-HDBK-5D.⁴ The findings compare favorably with typical results for 7075-T6X and generally exceed the set of established target goals. High-strength levels in the longitudinal extrusion direction (ultimate of 80-90 ksi and yield of 80-83 ksi) were obtained for the LOCKALITE alloy, along with tensile elongations of 7-9%. The fracture toughness of this IM Al-Li-X alloy was also determined for the -T8X temper using compact-tension (CT) test specimens. Preliminary toughness indications exceeded 30.0 ksi-in.^{1/2} in the L - T orientation. The strength/ductility/toughness combination for the LOCKALITE extrusion appears to be suitable for consideration as a replacement in structural applications involving conventional 7075-T6X Al alloy products.

**A. LOCATION OF TENSILE COUPONS CUT FROM 1.0 X 4.0 INCH EXTRUSION IN THE LT GRAIN ORIENTATION****B. LOCATION OF TENSILE SPECIMENS CUT FROM MID-THICKNESS OF 1.0 X 4.0 INCH EXTRUSION IN LONGITUDINAL GRAIN ORIENTATION****Fig. 3 Location of tensile and lug specimens in the 1.0 x 4.0-in. Al-Li-X extrusion.****Fig. 4 Tapered lug test specimen.**

Structural Tests

Specimen and Test Arrangements

Coupons were cut from the 1.0 x 4.0-in. extrusion to determine the variation in tensile and shear properties for the material used in the lug specimens. The locations of the test specimens and specimen identification numbers are shown in Fig. 3. Eight longitudinal (L) and four long-transverse (LT) specimens were cut from material near the lug material location. Four other longitudinal specimens (1-4) were taken near one end of the extrusion. All longitudinal specimens and three lug specimens were made from the middle one-inch thickness of the extrusion. Two of the long-transverse specimens were taken near the surface and two were taken near the middle of the one-inch thickness. Cylindrical double-shear-type specimens were also taken from the center section of the extruded bar. Triplicate shear tests were conducted for each of the orthogonal directions, L , LT , and ST .

The average results of the tensile and shear tests with respect to extrusion direction and location are compared in Table 2 with 7075-T6 extruded bar. These data show considerable variation in properties with respect to extrusion direction and location. There is about a 15-ksi difference in tensile strength between longitudinal surface specimens and long-transverse center specimens. Additionally, a 20% dif-

ference in shear strength is observed in the Al-Li-X extrusion as a function of specimen orientation. As shown in Table 2, the midsection tensile and shear properties of the Al-Li extrusion are comparable to the properties of 7075-T6 extruded bar.

Three tapered lug specimens were fabricated from the mid-thickness of the 1.0×4.0-in. Al-Li-X extrusion. The lug specimens were made to the configuration shown in Fig. 4. This specimen configuration was selected because finite-element stress analysis was available for lugs loaded at angles of 0, 45 and 90 deg to the lug axis.⁵ Therefore, the test results can be compared with predictions using the methods of analysis given in Ref. 6.

One of the lugs was tested at a loading angle of 0 deg with respect to the lug axis. The test was conducted in a universal test machine with a load range of 60,000 lb. Load was applied through a 180–200 ksi steel clevis and a 260–280 ksi steel pin that was used by Kathiresan et al.⁵ No bushing was used in the lug for this test.

One lug each was tested at loading angles of 45 and 90 deg in the test setups shown in Fig. 5. These are the same test arrangements that were used for the fatigue and crack-growth tests reported in Ref. 5. The pin and clevis was the same as was used for the lug test at a 0-deg loading angle. No bushings were used in either of these lugs.

Test Results

Figure 6 is a plot of the average bearing stress vs the normalized plastic deformation for each lug test to failure. The plastic deformation was measured in the same direction as the applied load for each specimen. Measurements made from all the tests were pieced together to obtain the continuous curves to failure; all three specimens failed at approximately the same ultimate load and deflection. The load-deflection characteristics of the lugs loaded at 0 and 45 deg were approximately the same. The larger deflection for the 90-deg loaded lug is probably due to an increase in bending deformation. The intersection of a vertical line at 0.002 in. with each curve in Fig. 6 would correspond to a yield load for a 0.2% offset. For these three tests, the yield load at a 0.2% offset was equal to 72, 77, and 58% of the ultimate load for loading angles of 0, 45, and 90 deg, respectively. These data indicate that the strength of lugs loaded at 90 deg would be limited by a yield strength criterion since the 0.2% offset is less than 67% of the ultimate load.

Photographs of the failed specimens are shown in Fig. 7. The plan view of the three small pieces that were broken off at failure in Fig. 8 shows the direction of loading, modes of failure, primary and secondary failure planes, and the predicted location of maximum tensile stress. The failure of all three lugs initiated in the primary failure plane near the location of the maximum tensile stress. The failure for all three specimens initiated on one side of the lug, followed by a secondary failure on the opposite side of the lug. The modes of failure, based on visual examination of the fracture surface, were identified as tensile mode or shear mode, as indicated in Fig. 8. The shear mode fracture surfaces were smoother and flatter than those of the tensile mode.

The primary failure planes did not precisely go through the point of maximum tensile stress. The predicted locations of maximum tensile stress are approximately the end points of the frictional contact between the pin and the lug. These peak stress locations can change under applied loading due to misalignment of the load axis, elongation of the hole, and bending deflection for the lugs loaded at angles of 45 and 90 deg. Also, the large difference in tensile properties between the *L*, *LT*, and *ST* orientations may have affected the location of primary failure.

The failure of the 90-deg loaded lug was very similar to previously reported failures obtained during fatigue testing of the 7075-T6 aluminum lugs of the same configuration.⁵ In the fatigue tests, cracks were initiated at the peak tensile

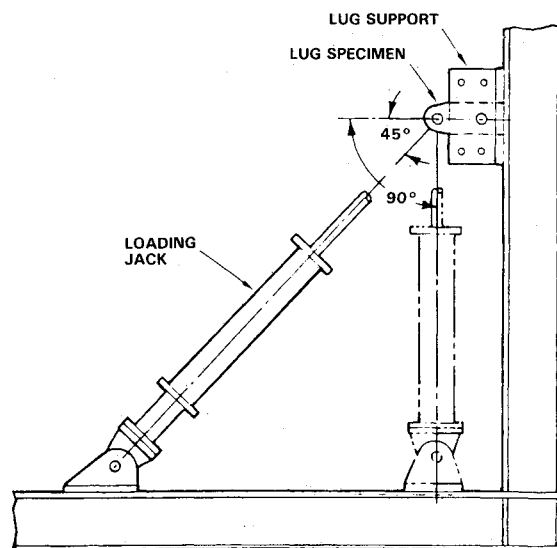


Fig. 5 Schematic of test setup for lugs located at angles of 45 and 90 deg.

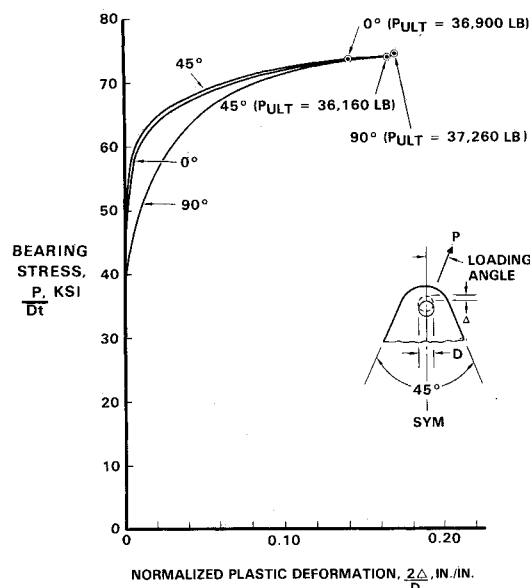


Fig. 6 Bearing stress vs normalized plastic deformation.

stress location. During crack propagation, the failure followed a path very similar to that shown in Fig. 8. Final failure is identified as the secondary tensile mode failure in Fig. 8c.

Comparison of Predictions and Test Results

The failure load for each lug was compared with the predicted load using the method of analysis developed in Ref. 6. In this method of analysis, the failure load can be calculated from the following equation:

$$P_{ult} = K_{BR} D t F_{tux} \quad (1)$$

where F_{tux} is the material ultimate strength in the orientation of lowest strength.

The value of K_{BR} is uniquely related to the elastic tension stress concentration factor K_{tb} at the edge of the lug hole. Reference 6 presents curves to determine the elastic stress concentration factor for various lug geometries and from the value of K_{BR} as a function of K_{tb} . The method of analysis is

Table 3 Comparison of predicted load^a and test load for Al-Li pin loaded lugs

Loading angle, deg	Hole diameter, in.	Lug thickness, in.	Predicted load, lb	Test load, lb	Test load Predicted load
0	0.999	0.499	41,510	36,900	0.89
45	0.996	0.502	38,960	36,160	0.94
90	1.001	0.503	45,004	37,260	0.83
				Avg	0.89

^aBased on $F_{tu} = 76,400$ psi in LT orientation.

applicable to both tension- and shear-bearing-type failures. In Ref. 6, the predicted load was correlated with the test load for 263 lug tests made from 25 materials. The accuracy of the predictions varied from 19% below the test loads to 15% above, with an average of 0.3% below the test loads.

The correlation between the predicted load, using the Ref. 6 method of analysis, and the test load for the three Al-Li lugs is given in Table 3. The predictions were made using the material tensile properties in the LT orientation. All three lugs failed below the predicted load, with the average of the three tests being 11% below the predicted load. However, the correlation between the predicted load and test load is within the accuracy for predicting the lug static strength by the method of analysis given in Ref. 6.

The lower shear strength properties obtained in the ST orientation, as shown in Table 2, may account for the lug strengths being below predicted values. Tensile stresses in the L and LT orientations also produce shear stresses across the lug thickness. As indicated in Eq. (1), the tensile strength in the lowest orientations should be used for predictions. The shear strengths in the L and LT orientations are observed to be about 50% of the tensile strength. Based on this relationship, the tensile strength in the ST orientation would be approximately 66,000 psi. Using a tensile strength of 66,000 psi for predicting the lug strength would result in test load to predicted load ratios from 0.96 to 1.07, with an average of 1.02. These findings tend to confirm that the properties in the ST orientation should be used to predict the static strength of pin-loaded lugs fabricated from Al-Li alloy extrusions.

Weight Savings Evaluation

Methodology

A weight-saving analysis was conducted using the methodology given in Ref. 7. The analysis uses the basic material mechanical properties to assess the weight savings for structural members sized to different failure modes. The aircraft structure is then separated into the various failure mode categories to determine the potential weight savings for the complete airframe.

Material Property Comparisons

Table 4 presents the material properties that are used to compare the weight savings for aluminum-lithium material as a replacement for 7075-T6X. Based on test data presented above, it is assumed that the design strength properties are equivalent for the two materials. However, aluminum-lithium alloy has a higher modulus of elasticity and a lower density than 7075-T6X material.

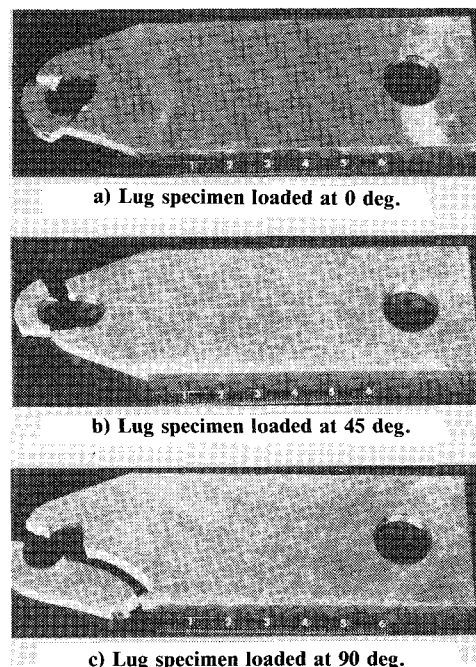
$$\text{Percent weight savings} = (1 - W_2/W_1) 100 \quad (2)$$

where W_1 = structural weight of baseline material and W_2 = structural weight of replacement material.

Therefore, weight savings from 7 to 17% are obtainable for these seven failure mode categories, as shown in Table 5.

Table 4 Material properties for weight-savings analysis

Material property	7075-T6X baseline	Aluminum lithium
Tensile strength, ksi	76	76
Compression yield, ksi	67	67
Modulus of elasticity, 10^6 psi	10.4	11.6
Density, lb/in. ³	0.101	0.094

**Fig. 7 Photographs of lug specimens after failure.**

The weight ratios W_2/W_1 for each failure mode category are calculated using the material properties given in Table 4 and the equations given in Table 5. For failure mode category 3, the secant modulus of elasticity is assumed to be equal to the Young's modulus of elasticity. The percent weight savings for each failure mode can be calculated from Eq. (2).

Potential Weight Savings for Al-Li-X Alloys

The weight savings for a complete aircraft is calculated by multiplying the percent weight saved for each failure mode by the percentage of the aircraft structure sized by that failure mode. This is an estimate, as the effect of secondary failure modes, with positive margins of safety, are not considered.⁷ The results of this analysis for a distribution of structural weight applicable to a fighter aircraft⁷ are given in

Table 5 Percent weight savings for various failure modes

Category no.	Failure mode	Weight ratio $\frac{W_2(\text{Al-Li})}{W_1(7075\text{-T6X})}$	Weight saving, %
1	Tensile strength	$\frac{\rho_2}{\rho_1} \frac{F_{tu1}}{F_{tu2}}$	7
2	Compressive strength	$\frac{\rho_2}{\rho_1} \frac{F_{cy1}}{F_{cy2}}$	7
3	Crippling	$\frac{\rho_2}{\rho_1} \left[\frac{E_{s1}}{E_{s2}} \right]^{0.25} \left[\frac{F_{cy1}}{F_{cy2}} \right]^{0.25}$	9
4	Compression surface column and crippling	$\frac{\rho_2}{\rho_1} \left[\frac{E_1}{E_2} \right]^{0.4} \left[\frac{F_{cy1}}{F_{cy2}} \right]^{0.2}$	11
5	Buckling compression or shear	$\frac{\rho_2}{\rho_1} \left[\frac{E_1}{E_2} \right]^{0.33}$	10
6	Aeroelastic stiffness	$\frac{\rho_2}{\rho_1} \frac{E_1}{E_2}$	17
7	Durability and damage tolerance assessment cutoff (DADTA)	$\frac{\rho_2}{\rho_1} \frac{F_1}{F_2}$	7

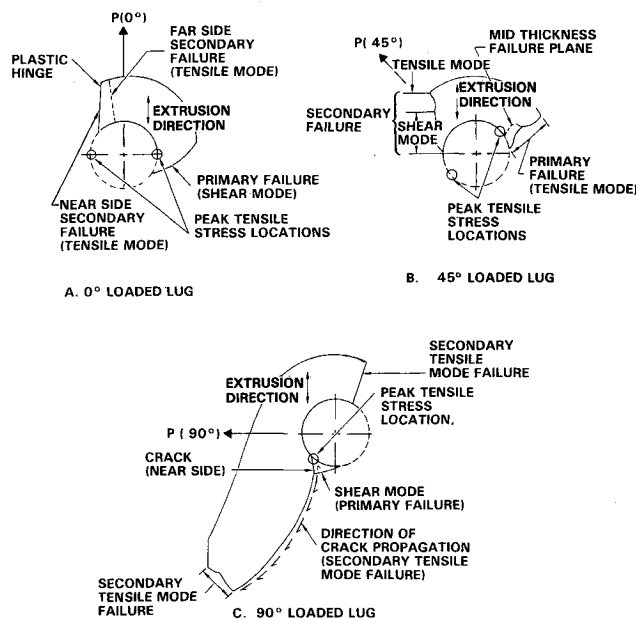


Fig. 8 Plan view of failed pieces from three lug specimens.

Table 6. These results indicate a potential weight savings of 9.5%. If an alloy with higher strength properties can be developed, then additional weight savings can be realized.

Conclusions

A materials mechanical properties and structural performance study on Al-Li-X alloys has been described in the preceding sections. The following conclusions are made:

1) The mechanical property behavior of the candidate Al-Li-X alloy (designated LOCKALITE) makes it a suitable

Table 6 Summary of weight savings for a fighter aircraft for Al-Li compared to 7075-T6X

Failure mode category	Fighter total weight, %	Weight saved, %
1	18.6	1.30
2	3.5	0.25
3	19.5	1.76
4	9.7	1.07
5	18.1	1.81
6	11.6	1.97
7	19.0	1.33
Totals	100.0	9.49

replacement for conventional 7075-T6X aluminum alloys (based on mechanical design conditions only). Other design conditions also need to be considered, such as fatigue, corrosion, stress corrosion, etc.

2) The results of tapered lug tests on the Al-Li-X alloy are consistent with prediction methods involving stress analyses and the mechanical properties in extrusion orientation with the lowest strength.

3) Consideration of failure mode criteria enables a calculation of potential weight savings from 7 to 17% for individual Al-Li aircraft structural components and 9.5% for a fighter aircraft.

References

- Lewis, R.E., Webster, D., and Palmer, I.G., "A Feasibility Study for Development of Structural Aluminum Alloys from Rapidly Solidified Powders for Aerospace Structural Applications," Interim Technical Report, June 1977 to July 1978, AFML-TR-78-102, July 1978.
- Chellman, D.J., Rainen, R.A., Divecha, A.P., and Garrett, R.K. Jr., "Influence of Solute Content on Properties of IM Al-Li-Cu-Mg-Zr Alloys," Presented at WESTEC Conference, Los Angeles, CA, March 1984.

³Chellman, D.J. and Rainen, R.A., "Influence of Composition and Processing Variables on Property Behavior of an IM Al-Li-Cu-Mg-Zr Alloy (LOCKALITE)," Presented at Third International Aluminum-Lithium Conference, Oxford, England, July 1985.

⁴*Metallic Materials and Elements for Aerospace Vehicle Structures*, Military Standardization Handbook MIL-HDBK-5D, June 1983.

⁵Kathiresan, K., Brussat, T.R., and Hsu, T.M., "Advanced Life

Analysis Methods—Crack Growth Analysis Methods for Attachment Lugs," AFWAL-TR-3080, Vol. II, Sept. 1984.

⁶Ekvall, J.C., "Static Strength Analysis of Pin Loaded Lugs," *Journal of Aircraft*, Vol. 23, May 1986, pp. 438-443.

⁷Ekvall, J.C., Rhodes, J.E., and Wald, G.G., "Methodology for Evaluating Weight Savings from Basic Material Properties," *Design of Fatigue and Fracture Resistant Structures*, ASTM STP-761, 1982, pp. 328-341.

From the AIAA Progress in Astronautics and Aeronautics Series . . .

AERO-OPTICAL PHENOMENA—v. 80

Edited by Keith G. Gilbert and Leonard J. Otten, Air Force Weapons Laboratory

This volume is devoted to a systematic examination of the scientific and practical problems that can arise in adapting the new technology of laser beam transmission within the atmosphere to such uses as laser radar, laser beam communications, laser weaponry, and the developing fields of meteorological probing and laser energy transmission, among others. The articles in this book were prepared by specialists in universities, industry, and government laboratories, both military and civilian, and represent an up-to-date survey of the field.

The physical problems encountered in such seemingly straightforward applications of laser beam transmission have turned out to be unusually complex. A high intensity radiation beam traversing the atmosphere causes heat-up and breakdown of the air, changing its optical properties along the path, so that the process becomes a nonsteady interactive one. Should the path of the beam include atmospheric turbulence, the resulting nonsteady degradation obviously would affect its reception adversely. An airborne laser system unavoidably requires the beam to traverse a boundary layer or a wake, with complex consequences. These and other effects are examined theoretically and experimentally in this volume.

In each case, whereas the phenomenon of beam degradation constitutes a difficulty for the engineer, it presents the scientist with a novel experimental opportunity for meteorological or physical research and thus becomes a fruitful nuisance!

Published in 1982, 412 pp., 6×9, illus., \$29.50 Mem., \$59.50 List

TO ORDER WRITE: Publications Dept., AIAA, 1633 Broadway, New York, N.Y. 10019